Fluorescence of polyaniline films on electrode surfaces: Thickness dependence and surface influence

P. Soledad Antonel, Estela M. Andrade, Fernando V. Molina *

INQUIMAE, Facultad de Ciencias Exactas y Naturales, Universidad de Buenos Aires, C. Universitaria, Pabellon II, Buenos Aires C1428EHA, Argentina

ABSTRACT

The dependence of the photoluminescence of polyaniline films, supported onto platinum or fluorine-doped SnO_2 (FTO) electrodes, on the film thickness (as measured by the voltammetric charge) has been studied for different polymer oxidation states. The fluorescence emission spectra have been corrected for absorption and reflection from the underlying metal surface. For platinum electrodes, the absolute quantum yield for films of different thicknesses, and at several electrode potentials, has been obtained using as reference anthracene in acrilic films. Also, the corrected emission for growing films at different charges was recorded. The potential dependence of the emission intensity is not affected by the film thickness. The corrected emission intensity on FTO surfaces increases linearly with thickness due to the increase in the number of fluorophores. In the case of Pt, the intensity is null for low thicknesses, quenched by the metallic surface; as the thickness increases beyond a critical value, the emission increases sharply and then reduces its slope increasing more slowly. The quantum yield on Pt surfaces is accordingly zero for sufficiently thin films, and then increases in a nearly linear way. The observed behaviour on metal surfaces is found to be due to the interference between the field of the emitting dipole and the surface reflected field, causing vanishing emission for dipoles sufficiently near to the surface, and a complex distance dependence afterwards. The theoretical model is found to agree with the experiments if a distribution of parallel and perpendicular dipoles is introduced, with dipoles near the surface being predominantly parallel.

© 2009 Elsevier B.V. All rights reserved.

1. Introduction

Aryl amine conducting polymers, such as polyaniline (PANI), show interesting optical properties (such as electrochromism and fluorescence) leading to a number of proposed applications such as sensors, displays and other optoelectronic devices [1–13]. PANI and similar polymers show photoluminescence in their reduced state, which decreases when the polymer is oxidized [14–19]. Even when the quantum yield is small, the study of these properties is interesting because it will give insight into the electronic structure of these materials. There are relatively few studies concerning the photoluminescence of PANI and similar polymers. Son et al. [14] studied the fluorescence quenching of PANI upon oxidation, and developed a simple model assuming that charge carriers (polarons) are responsible for quenching, allowing for overlapping between quenching centers. Thorne et al. [15] studied the time-resolved fluorescence of the reduced form of PANI, leucoemeraldine (LE), and explained the time decay curves as due to the diffusion in one dimension of randomly located traps, postulated to be short

segments of the oxidized, emeraldine (EM), form of PANI. Shimano and MacDiarmid [17] studied the influence of oxidation state and hydration degree on the fluorescence of PANI, both in N-methylpyrrolidinone (NMP) solutions and as glass supported films: they observed the decrease in emission intensity as the polymer is oxidized, and found a dependence with the amount of water present (humidity); the results were interpreted considering PANI as a dynamic block copolymer.

The redox switching of PANI and similar polymers are usually interpreted in terms of two redox states, the reduced leucoemeraldine and half oxidized emeraldine, the conversion between them being a two-electron reaction [1–3,18–24]. It involves an intermediate state (radical cation or polaron), which shows unpaired spins in EPR measurements [25–27] and has been considered to be a transient one. However, more recently it has been considered as a stable state called protoemeraldine (PE), explaining the temperature dependence of the PANI magnetic susceptibility in terms of the LE–PE–EM equilibrium [27]. The same scheme was successfully applied to explain the electrochemomechanical behaviour of thick PANI films [28], considering the presence of a distribution of formal redox potentials for the PE to EM oxidation [29–31]. From a structural point of view, it has been proposed [32] and recently shown [33,34] that in the conductive (doped emeraldine) state,

* Corresponding author. Tel.: +54 11 4576 3378/80x119/230; fax: +54 11 4576 3341.

E-mail address: fmolina@qi.fcen.uba.ar (F.V. Molina).

PANI films are actually composed of small, highly interacting, quasi-crystalline, conductive domains separated by low conductivity regions; it has been also proposed [35] that conduction is achieved through resonance tunneling between the conductive domains.

More recently [36,37], the fluorescent emission of PANI in different redox states was studied, measuring the quantum yield of the base forms of LE and EM in solution with NMP as solvent. The leucoemeraldine base spectrum in NMP shows an emission maximum at a wavelength λ_{em} = 384 nm. The corresponding emeraldine base form shows a maximum at the same position, but with a slightly low intensity [36]. The quantum yield for both forms were found to be ϕ_{LE} = 1.2 × 10^{-3} and ϕ_{EM} = 1.0 × 10^{-3}. The fluorescence of PANI films supported on platinum electrodes was also studied [36]. In the case of PANI films in the base form, it was found that the spectra are noticeably shifted to higher wavelength compared with NMP solution, having maximum intensity at 412 nm in the EM base form and about 450 nm for the LE base form. Moreover, the EM base spectrum has much lower intensity than the LE base one, as it was found in NMP solution. In the case of PANI films in the salt form, for small thicknesses no emission was observed; as the film thickness increased, the observed intensity increased, reached a maximum and afterwards decreased slightly. The fluorescent behaviour of PANI films as a function of applied potential was also studied [37], applying a correction to account for absorption in the film and reflection at the metal surface. It was observed a decrease in emission intensity as the polymer film is oxidized (going from 0.1 to 0.6 V vs. RHE), leaving a small but not null emission when the polymer is in the emeraldine state. Also, it was found that the relative quantum yield decreases to a minimum but finite value when the polymer is oxidized to EM. This behaviour was interpreted considering the oxidation states LE, PE and EM, the three states having different spectroscopic behaviour, and a film structure composed of quasi-crystalline domains separated by disordered regions, the emission being efficiently quenched in or near those ordered domains.

In this work the thickness and surface nature dependences of the quantum yield of PANI films supported on platinum and fluorine-doped tin oxide (FTO) electrodes are studied at different electrode potentials. The fluorescent emission is measured, corrected for absorption and the absolute quantum yields are obtained. The quantum yield dependence with film thickness is analyzed.

2. Materials and methods

2.1. Electrosynthesis of polymer films onto electrodes

AR grade chemicals and high-purity water from a Milli Q system were employed. Aniline was distilled under reduced pressure and reducing conditions shortly before use. PANI films were synthesized electrochemically from 0.1 M aniline in 1 M sulfuric acid solutions. A Teq-03 potentiostat under computer control was employed. Both the electropolymerization and the fluorescence experiments were conducted in a specially constructed cell, allowing to perform electrochemical processes with simultaneous fluorescence or absorbance measurements [37]. It is a rectangular cell (5.94 cm × 9.03 cm, wall thickness 0.50 cm), made of high density polyethylene. The working electrode had a rectangular shape, with a surface area of about 1 cm^2, and was either a platinum plate or a FTO covered glass mounted on a rotatory holder in order to adjust the incidence angle. The FTO electrode has a resistance of 21–25 Ω/□. The metallic electrode was polished with alumina slurries of successively smaller particle sizes down to 0.05 μm, washed in an ultrasonic bath, and rinsed with ultrapure water. A platinum auxiliary electrode (CE) was placed in a compartment separated by a porous glass, to avoid contamination of the working electrode

solution with CE products; this compartment was filled with the same solution as the main one. The reference electrode was a reversible hydrogen one (RHE) in the same solution with the working electrode. The solution was deoxygenated with N$_2$ for about 15 min, before the electrochemical measurements. The electropolymerization was performed by potential cycling between 0.05 and 1.00 V at a scan rate, v, of 0.050 V s^{-1}. Before each experiment, the working electrode was soaked in sulphonitric mixture and rinsed thoroughly. The potentials were converted to and are presented on the standard hydrogen electrode scale (SHE). The polymerization was monitored through the total voltammetric reduction charge, Q_{tot}, in the full polymerization potential range, and was stopped at different Q_{tot} values, in order to obtain films of different thicknesses.

2.2. Fluorescence measurements

2.2.1. Fluorescence intensity corrections and quantum yield determination

As discussed previously [37], in the analysis of photoluminescence of solid films, it must be considered the absorption of both the excitation and emission beams by the film material, as well as the reflective properties of the supporting surface in order to have quantitatively correct results. When a fluorescent film of thickness L, supported on a reflective surface, is irradiated with an excitation beam of intensity I_0 (of wavelength λ_0), the corrected emission intensity $I_{m,c}$ is related to the intensity measured at the detector I_m, at a given emission wavelength λ_e, by

$$I_{m,c} = I_m \left\{ \frac{1}{\left(\frac{\alpha_0 L}{\cos\theta_0} + \frac{\alpha_e L}{\cos\theta_e}\right)} \left[1 - \exp\left(-\frac{\alpha_0 L}{\cos\theta_0} - \frac{\alpha_e L}{\cos\theta_e}\right) \right] \right.$$
$$+ \frac{f_e \exp\left(-\frac{2\alpha_e L}{\cos\theta_e}\right)}{\left(\frac{\alpha_0 L}{\cos\theta_0} - \frac{\alpha_e L}{\cos\theta_e}\right)} \left[1 - \exp\left(-\frac{\alpha_0 L}{\cos\theta_0} - \frac{\alpha_e L}{\cos\theta_e}\right) \right]$$
$$+ \frac{f_0 \exp\left(-\frac{2\alpha_0 L}{\cos\theta_0}\right)}{\left(-\frac{\alpha_0 L}{\cos\theta_0} + \frac{\alpha_e L}{\cos\theta_e}\right)} \left[1 - \exp\left(\frac{\alpha_0 L}{\cos\theta_0} - \frac{\alpha_e L}{\cos\theta_e}\right) \right]$$
$$\left. + \frac{f_0 f_e \exp\left(-\frac{2\alpha_0 L}{\cos\theta_0} - \frac{2\alpha_e L}{\cos\theta_e}\right)}{\left(\frac{\alpha_0 L}{\cos\theta_0} + \frac{\alpha_e L}{\cos\theta_e}\right)} \left[\exp\left(\frac{\alpha_0 L}{\cos\theta_0} - \frac{\alpha_e L}{\cos\theta_e}\right) \right] - 1 \right\}^{-1}$$

(1)

where f_0 and f_e are the metal reflectance values at λ_0 and λ_e respectively, α_0 and α_e are the respective absorption coefficients, θ_0 is the incidence angle of I_0 and θ_e is the angle of emission [37]. For platinum supported films, Eq. (1) was applied in order to obtain the corrected intensity. For FTO supported films, the reflectance was considered negligible so that Eq. (1) simplifies considerably to:

$$I_{m,c} = I_m \left\{ \frac{1}{\left(\frac{\alpha_0 L}{\cos\theta_0} + \frac{\alpha_e L}{\cos\theta_e}\right)} \left[1 - \exp\left(-\frac{\alpha_0 L}{\cos\theta_0} - \frac{\alpha_e L}{\cos\theta_e}\right) \right] \right\}^{-1} \quad (2)$$

For FTO supported films Eq. (2) is applicable; however, it must be taken into account that there is some emission from the FTO film in the wavelength range studied. This emission (and the corresponding excitation) is affected by the absorption in the polymer, thus the correction applied for FTO supported PANI films was:

$$I_{m,c} = (I_m - T_{PANI}(\lambda_0) T_{PANI}(\lambda_e) I_{FTO,0})$$
$$\times \left\{ \frac{1}{\left(\frac{\alpha_0 L}{\cos\theta_0} + \frac{\alpha_e L}{\cos\theta_e}\right)} \left[1 - \exp\left(-\frac{\alpha_0 L}{\cos\theta_0} - \frac{\alpha_e L}{\cos\theta_e}\right) \right] \right\}^{-1} \quad (3)$$

where T_{PANI} is the transmittance of the PANI film at each wavelength and $I_{FTO,0}$ is the intensity measured for the bare FTO surface.

Absolute quantum yields can be determined if a suitable reference of known quantum yield is measured in the same conditions as the sample. In this case, anthracene contained in films of poly(methylmethacrilate) supported on platinum were used; the quantum yield of anthracene in these films is known to be ϕ = 0.24 [38]. The films were deposited by spin coating from chloroform solutions and their emission measured immediately after measuring that of the PANI films.

First of all, by integration of the corrected emission spectra (for both, PANI and reference), the total emission intensity (I_{tot}) was obtained:

$$I_{tot} = \int I_{m,c} d\lambda \tag{4}$$

Then, the quantum yield is obtained as

$$\phi_{PANI} = \phi_{anth} \frac{A_{anth}}{A_{PANI}} \frac{I_{tot,PANI}}{I_{tot,anth}} \tag{5}$$

where anth indicates anthracene and A is the absorbance at λ_0. For the anthracene containing films, because the absorbance was very low, the correction of Eq. (1) reduces to

$$I_{m,c} = I_m \left\{ \frac{1}{1 + f_e + f_0 + f_0 f_e} \right\} \tag{6}$$

Thus, in (5) the PANI emission, corrected using Eq. (1), is integrated over the measured wavelength range, whereas the anthracene emission is integrated in the same range after correction by Eq. (6). Absorbance and reflectance measurements were also conducted in order to obtain the correction parameters.

2.2.2. Fluorescence of PANI films at different potentials and thicknesses

The thickness dependence was measured in two ways: in the first case, separate films of different thicknesses were prepared on platinum and the absolute quantum yields at different potentials determined as described in Section 2.2.1. The second way was to measure the emission of the same film at different thicknesses in the reduced state, by stopping the electropolymerization and holding the potential at the cathodic limit. Here, both Pt and FTO electrodes were employed.

In the first case, the working electrode was extracted after polymerization from the cell and carefully rinsed with high-purity water. The cell was then filled with 1 M sulfuric acid, and voltammetric cycling was performed between 0.05 and 0.60 V, at 0.050 V s^{-1}. The voltammetric reduction charge in that potential range, in supporting electrolyte solution (from EM to LE), Q, was recorded as a measure of film thickness; although the thickness could be estimated from Q through ellipsometric measurements [39], the relationship between them is dependent on polymerization conditions, thus for the experiments reported here the charge will be given. For PANI films electropolymerized in H$_2$SO$_4$, it is estimated that a 19 mC cm^{-2} film (charge measured between 0.60 and 0.05 V) has a thickness of 200 nm [39]. The emission spectra were recorded at potentials between 0.1 and 0.6 V. At each applied potential, the spectrum was recorded when the current (absolute value) was below 1 μA cm^{-2}. The time required was about 15 min at each potential, and it was determined by chronoamperometric measurements. The response of the bare Pt surface was also observed.

In the second case (same film at different thicknesses) the protocol utilized for the measurements on platinum was as follows:

- Five cycles were conducted from 0.05 to 1.00 V, and polymerization was stopped at 0.05 V.

- Stabilization of the system, until the current was below 1 μA cm^{-2}.
- Measurement of the fluorescence emission spectrum (always at a E = 0.05 V), with λ_0 = 310 nm, and emission range from 330 to 600 nm.
- These steps were repeated until a maximum charge was reached.

In the case of FTO surfaces, the protocol was somewhat different. First, the number of polymerization cycles between fluorescence measurements was incremented to 10–15, because the polymerization of aniline on FTO substrates is slower than on Pt electrodes. Then, λ_0 was set at 340 nm, with a emission range from 360 to 600 nm. The excitation wavelength was changed because a slight displacement of the absorption band was noticed.

It should be mentioned that the charge values Q, measured between 0.05 and 0.60 V, were obtained during the polymerization. Cyclic voltammetry in support electrolyte alone was not performed, because the necessary handling of the electrochemical cell could led to modifications of the position and/or orientation of the working electrode, introducing uncertainties in the measurements of fluorescence. For the same reason, no measurement of fluorescence reference was carried out.

The fluorometric measurements were performed using a PTI Quantamaster stationary spectrofluorometer. The incidence angle was set at 30°, to avoid direct reflection of the excitation beam into the photomultiplier.

2.3. Absorption spectra of PANI films

For the absorbance measurements of metal-supported PANI, semitransparent gold films 40 nm thick were deposited by evaporation onto quartz windows, and their absorption spectra in the range 310–600 nm were recorded. For FTO supported polymer, the absorbance of the FTO covered glass was measured in the same range. Then, PANI films were electropolymerized as described above, and their absorption spectra were recorded potentiostatically at potentials between 0.1 and 0.6 V, in the same conditions as for the fluorometric experiments. In all cases the absorbance of the bare gold or FTO film was subtracted. All the absorbance spectra were obtained using a Hewlett–Packard 8452A diode array spectrophotometer with the same cell described previously [36].

2.4. Reflectance spectra of platinum electrodes

The total reflectance of the platinum electrodes, polished as described above, was measured in the range 310–600 nm using a Shimadzu PC-3101 spectrophotometer equipped with a ISR-260 reflectance accessory, using BaSO$_4$ as standard.
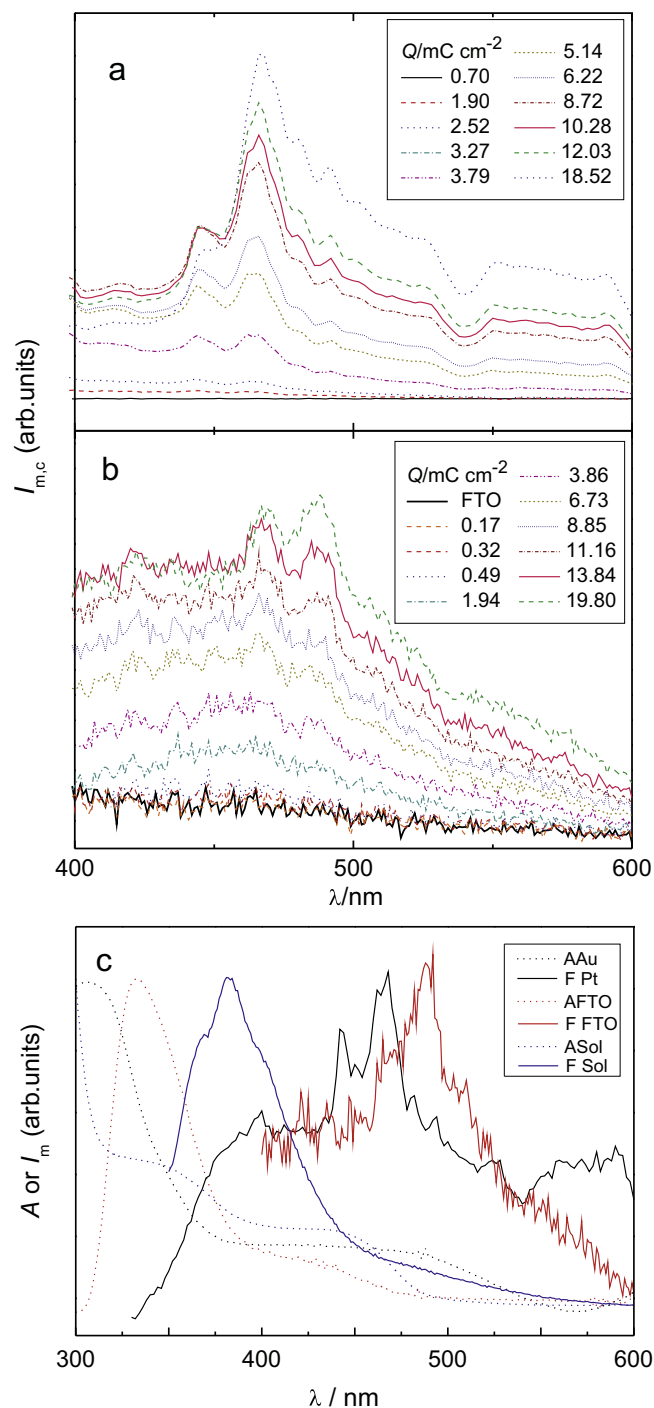
3. Results and discussion

Fig. 1 shows cyclic voltammograms recorded during the electropolymerization of aniline on Pt (a) and FTO (b). In the case of platinum, the voltammograms have the features already described by several authors [1–5,18–21]. In the case of FTO, the effect of the FTO film resistance is noticeable; as a result, the electropolymerization on this material was slower than on platinum. Otherwise, the films had the same properties and behaviour on both surfaces. In general, up to approximately 90 polymerization cycles were performed on platinum, and about 250 on FTO. These numbers correspond to thicknesses beyond which the absorbance was so high as to preclude computation of the corrected emission with a reasonable degree of accuracy.
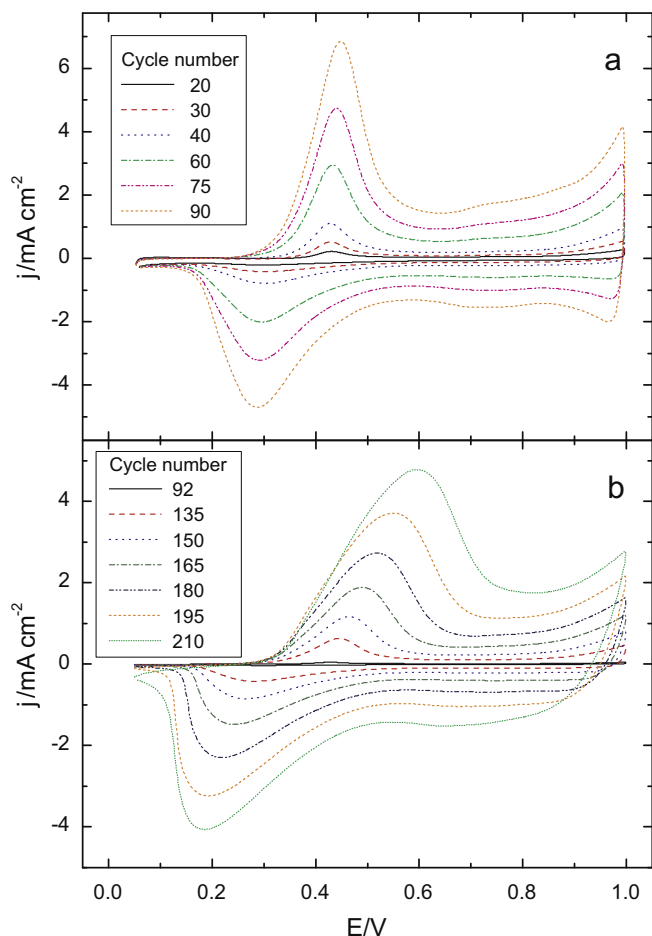
Fig. 1. Cyclic voltammograms during the electropolymerization of aniline on: (a) Pt and (b) FTO surfaces. 0.1 M aniline in 1 M H_2SO_4. 0.050 V s^{-1}.

Fig. 2. Emission spectra for PANI films at $E = 0.05$ V in 1 M H_2SO_4 on: (a) platinum and (b) FTO electrodes for different thicknesses (indicated by the voltammetric charge Q, measured between 0.60 and 0.05 V). (c) Emission and absorption spectra for PANI films, in leucoemeraldine state, on different substrates: (A) absorbance (F), fluorescence intensity. Au, PANI supported on gold thin films deposited on quartz. Pt, PANI films supported on Pt solid electrodes. FTO, PANI films on FTO film–covered glass substrates. Sol, in NMP solution (in base form, PANI salt form is not soluble).

Fig. 2 shows the corrected fluorescence emission spectra of a PANI film on Pt (a) and FTO (b) at the cathodic potential limit (0.05 V) for different charges Q during the electropolymerization. In (b) the emission spectrum of FTO is also presented; it is observed that for small thicknesses the emission in the presence of PANI is the same as of FTO alone (i.e., no polymer emission is observed). In the case of films supported on Pt, the corrected fluorescence emission spectra were obtained from the experimental spectra through Eq. (1), after subtracting the metal dispersion background, using the absorption spectra and the platinum reflectance spectrum (not shown). Because the Pt dispersion intensity was very low, it was subtracted directly, not attempting a correction like Eq. (3). In the case of films supported on FTO, the spectra were corrected through Eq. (3). Fig. 2c compares the PANI emission and absorption spectra on metal and FTO surfaces, as well as those in N-methylpirolidinone (NMP) solution in base form (the salt form is not soluble). It should be noted that the absorption spectra are coincident with those reported previously [36,37]; in particular, absorbance spectra on FTO surfaces were coincident in shape with those measured on Au surfaces. Cruz and Ticianelli [39] reported that the refractive index of PANI films is approximately 1.5, close to that of water, and because PANI films are porous and incorporate electrolyte [28], it is assumed that the PANI refractive index is approximately equal to that of the external medium (aqueous solution), thus no corrections are required for the incidence and emission angles.

It is observed that the intensity increases as the film grows, but also it is noticed in the case of platinum that the band shape changes, increasing more at wavelengths above 450 nm. Moreover,

the emission band for both electrodes is centred at the same wavelength range (between 450 and 500 nm). This indicates that the emission state is not altered by the different supports, in spite of the different shape of the bands. As it was indicated previously [36,37], the peaks observed in the fluorescence spectra are due to Raman dispersion from the underlying surface.

By integration of the corrected emission spectra, the total emission intensity (I_{tot}) was obtained and is presented in Fig. 3. In the
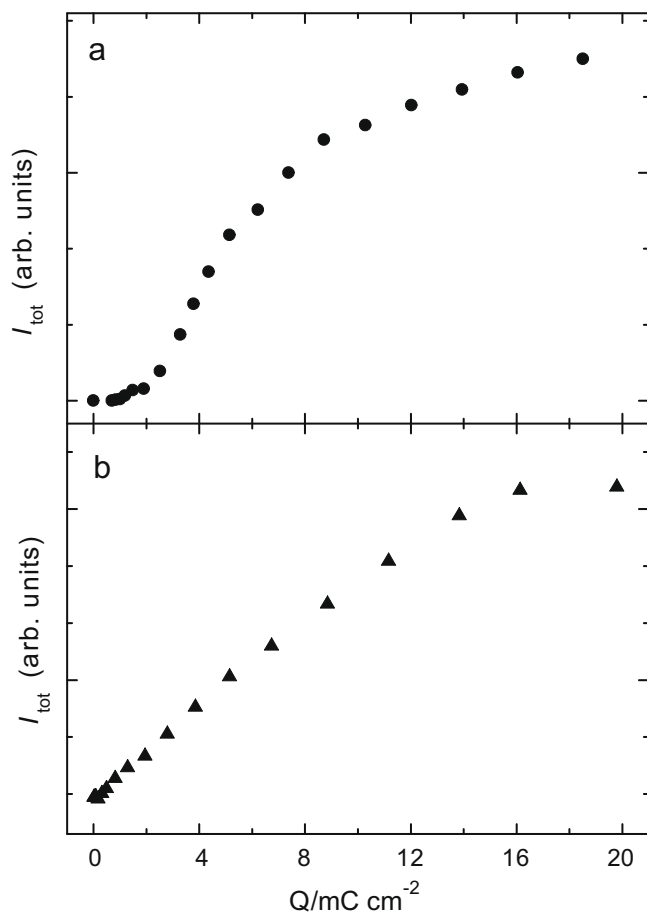
Fig. 3. Total corrected emission for PANI films at $E = 0.05$ V in 1 M H_2SO_4 on: (a) platinum and (b) FTO electrodes for different thicknesses (indicated by the voltammetric charge Q, measured between 0.60 and 0.05 V).

case of films supported on Pt (Fig. 3a), no emission is observed for low charges, Q, (film thicknesses), as it was reported earlier [36]. This is due to the interaction with the metallic surface (platinum electrode), as it will be analyzed later. Beyond a critical thickness, the emission increases sharply and then continues increasing but with a lower slope. In the case of films supported on FTO
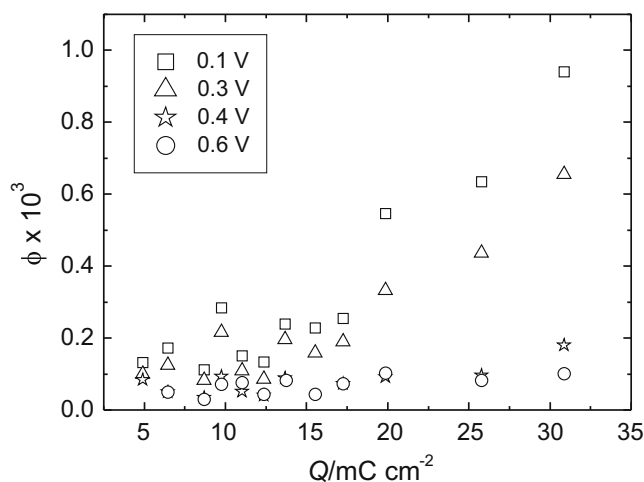
Fig. 4. Fluorescence quantum yield for PANI films in 1 M H_2SO_4 as a function of the thicknesses (measured by the voltammetric charge Q at different potentials in 1 M H_2SO_4).

(Fig. 3b), I_{tot} increases linearly from low Q values, so the metallic effect is not present. This dependence is due to the increase in the number of fluorophores as the film thickness increases. Then, the total emission intensity appears to approach a plateau; due to the absorbance increase, which is very high in this film thickness range, introducing an important error in its determination, this part of the curve should be taken with caution. Thus, within experimental error in the range studied, the corrected film emission on FTO increases linearly with film thickness.

Fig. 4 shows the absolute quantum yield, ϕ, of PANI films supported on Pt, calculated with Eq. (5), as a function of charge, Q, for different electrode potentials, E. At $E = 0.1$ V it is observed that the absolute quantum yield increases with film thickness, as it was presented in Fig. 3a. However, there are some differences. In Fig. 4 marked changes in slope with Q are not observed as in Fig 3a. Moreover, even through the experimental conditions were reproduced carefully, including the use of a fluorescence reference, the absolute quantum yield as a function of Q presents a relatively high dispersion, which can be attributed to the nature of aniline electropolymerization, being difficult to obtain exactly reproducible films.

The absolute quantum yields at $E = 0.1$ V are lower than those obtained in NMP solutions [36]; as it is observed in Fig. 4, the absolute quantum yields for PANI films varies approximately from 10^{-4} to 10^{-3} with increasing film thickness. In the case of the LE base form of PANI in NMP, $\phi = 1.2 \ 10^{-3}$ [36]; taking into account the behaviour observed in Fig. 3a, and noticing that the observed quantum yields are actually values averaged over the film thickness, it can be expected that the value observed in solution would be reached at somewhat higher thicknesses. Unfortunately, it could not be possible to reach this limiting value because (as discussed above) the higher the film thickness, the higher the absorbance, so the uncertainty introduced in the absolute quantum yield converts it in an unreliable value. However, it can be possible that the intrinsic quantum yield of the film (not counting the metal effect) is different from the one obtained in NMP solution. In the case of PANI films, the fluorescence spectra correspond to the salt form of the polymer, when in NMP solutions correspond to the base form, so the differences between them can be attributed to a different chemical environment (Fig. 2c). In NMP solution the ionic interactions are not present, because the polymer is in its neutral form, but in PANI films the polymer is in its salt form (positively charged), so it interacts with the anions of the support electrolyte (HSO_4^- and $SO_4^=$).

Another fact observed in Fig. 4 is that the quantum yield decays when the polymeric film is oxidized. Moreover, from $E = 0.4$ V the absolute quantum yield does not change noticeably with charge increase. So, the observed difference in the absolute quantum yields of the insulating ($E = 0.1$ V) and conducting ($E = 0.6$ V) forms of PANI is higher for thicker films. These results are in excellent agreement with those reported earlier [37], where the potential dependence of the fluorescence emission and of the relative quantum yields of films of different charges Q was studied. Finally, the general shape of the quantum yield–charge plots in Fig. 4 appears to be independent of potential (that is, the plots are approximately linear in the Q range, the slope being function of potential). So, the effect causing low quantum yields at lower charges (thicknesses) is independent of potential.

The fluorescence quenching at low thicknesses caused by the metal can be attributed to an electromagnetic effect due to the reflecting properties of the metal surfaces as follows. It was found by Drexhage et al. [40] that the fluorescence lifetime (and, hence, the emission efficiency) of an emitting molecule near a reflecting surface is a function of the distance between the molecule and the surface, due to the interference between the field of the emitting molecular dipole and the surface reflected field. The decrease
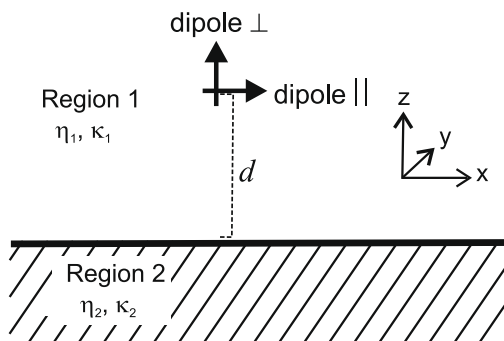
Fig. 5. Geometry of the metal/polymer system for the Chance et al. [41] theory.

in the lifetime when the distance becomes small is due to nonradiative transfer of energy from the excited molecule to the metal [41]. The emitting molecule acts as an oscillating dipole near a partially absorbing and partially reflecting surface. Chance et al. [42] developed a classical description of fluorescence and energy transfer from excited molecules to reflective surfaces. It should be noted that it was developed a quantum-mechanical treatment of lifetime variations [43,44], which is in complete agreement with the classical results. Here, we will apply the classic electromagnetic treatment to the thickness dependence of the quantum yield.

Fig. 5 shows the system geometry. Region 1 corresponds to the platinum electrode with dielectric constant ε_1, and region 2 to the polymer film with dielectric constant ε_2; $\varepsilon_i = (\eta_i + i\kappa_i)^2$, where η_i and κ_i are the respective real and imaginary parts of the refractive index. It should be noted that the analysis of Chance et al. corresponds to a fixed emission wavelength, λ_e, so each optical constant is evaluated at this λ_e. Finally, d is the distance between the dipole and the reflective surface. The method of Chance et al. gives a rigorous separation of two effects of a reflective surface: radiative and nonradiative energy transfer. It should be considered two types of dipoles: those oriented perpendicular to the interface, and those oriented parallel.

In the case of Fig. 5, if a plane above the dipole ($z > d$) and a plane below it ($0 < z < d$) are considered, the total energy flux through these planes can be obtained. The flux through each plane, $F_\uparrow$ or $F_\downarrow$, is calculated by integrating the normal component (**n**) of the complex Poynting vector, $\mathbf{S}^*$, over the plane:

$$F_{\uparrow,\downarrow} = \mathrm{Re} \int_{A\uparrow,\downarrow} \mathbf{S}^* \cdot \mathbf{n}\, dA \tag{7}$$

$$\mathbf{S}^* = \left(\frac{c}{8\pi}\right) E \times \mathbf{H}^* \tag{8}$$

$$\mathbf{H} = -i\left(\frac{\omega}{c}\right)\nabla \times \Pi \tag{9}$$

where **E** corresponds to the electric field at any point in region 1, **H** is the magnetic field, Π is the Hertz vector (which has a different expression for perpendicular and parallel dipoles), ω is the frequency and c is the speed of light.

Following Chance et al. [42] Eqs. (10)–(13) show the results for the normalized decay constants (inverse of the lifetime) $\hat{b} = b/b_0$ (where b_0 is the decay constant in the absence of the reflecting surface) for the emission through the above and below planes, for the perpendicular ($\hat{b}_\uparrow^\perp, \hat{b}_\downarrow^\perp$) and parallel ($\hat{b}_\uparrow^\parallel, \hat{b}_\downarrow^\parallel$) dipoles, respectively:

$$\hat{b}_\uparrow^\perp = q - \frac{3}{4}q\,\mathrm{Im}\int_0^1 (1 - |R^\parallel|^2)\frac{u^3\,du}{l_1} - \frac{3}{2}q\,\mathrm{Im}\int_0^1 R^\parallel \frac{e^{-2l_1\hat{d}}}{l_1}u^3\,du \tag{10}$$

$$\hat{b}_\downarrow^\perp = \frac{3}{4}q\,\mathrm{Im}\int_0^1 (1 - |R^\parallel|^2)\frac{u^3\,du}{l_1} - \frac{3}{2}q\,\mathrm{Im}\int_1^\infty R^\parallel \frac{e^{-2l_1\hat{d}}}{l_1}u^3\,du \tag{11}$$

$$\hat{b}_\uparrow^\parallel = q - \frac{3}{8}q\,\mathrm{Im}\int_0^1 \frac{u}{l_1}\left[(1 - |R^\perp|^2) + (1 - u^2)(1 - |R^\parallel|^2)\right]du$$
$$+ \frac{3}{4}q\,\mathrm{Im}\int_0^1 \frac{u}{l_1}e^{-2l_1\hat{d}}[R^\perp + (1 - u^2)R^\parallel]\,du \tag{12}$$

$$\hat{b}_\downarrow^\parallel = \frac{3}{8}q\,\mathrm{Im}\int_0^1 \frac{u}{l_1}\left[(1 - |R^\perp|^2) + (1 - u^2)(1 - |R^\parallel|^2)\right]du$$
$$+ \frac{3}{4}q\,\mathrm{Im}\int_0^1 \frac{u}{l_1}e^{-2l_1\hat{d}}\left[R^\perp + (1 - u^2)R^\parallel\right]du \tag{13}$$

Here, $R^\parallel$ is the reflection coefficient of an incident ray polarized parallel to the plane of incidence (p-polarized) and $R^\perp$ is the reflection coefficient for the incident ray polarized perpendicular to the plane of incidence (s-polarized):

$$R^\parallel = \frac{\varepsilon_1 l_2 - \varepsilon_2 l_1}{\varepsilon_1 l_2 + \varepsilon_2 l_1}, \quad R^\perp = \frac{l_1 - l_2}{l_1 + l_2} \tag{14}$$

In Eq. (14), l_1 and l_2 are defined as:

$$l_1 \equiv -i(1 - u^2)^{1/2}, \quad l_2 \equiv -i\left(\frac{\varepsilon_2}{\varepsilon_1} - u^2\right)^{1/2} \tag{15}$$

Finally, q is the relative emission in the absence of reflective surface and $\hat{d}$ is the normalized distance between the dipole and the surface:

$$\hat{d} \equiv \frac{2\pi(\eta_1 + i\kappa_1)}{\lambda}d \tag{16}$$

Now an apparent quantum yield at a given wavelength λ_e, q_a, can be calculated for both cases, perpendicular and parallel dipoles, as:

$$q_a^\perp = \frac{b_\uparrow^\perp}{b_{tot}^\perp} \tag{17}$$

$$q_a^\parallel = \frac{b_\uparrow^\parallel}{b_{tot}^\parallel} \tag{18}$$

$$b_{tot}^\perp = b_\uparrow^\perp + b_\downarrow^\perp + (1 - q) \tag{19}$$

$$b_{tot}^\parallel = b_\uparrow^\parallel + b_\downarrow^\parallel + (1 - q) \tag{20}$$

Fig. 6 shows calculated curves for $q_a^\perp$ and $q_a^\parallel$ at $\lambda_e = 500$ nm. The optical parameters employed were $\eta_1 = 1.5$; $\kappa_1 = 0$; $\eta_2 = 2.0$; $\kappa_2 = 3.4$. For PANI it was set $\kappa_1 = 0$ because, the experimental fluorescence emission was already corrected for the absorbance at λ_0 and λ_e. The results of Fig. 6 cannot be directly compared with the experiments, because they show the emission of dipoles at a fixed distance from the surface, thus these curves should be integrated to find the total emission (quantum yield) of a film of a given thickness. Moreover, it should be considered the relative contributions of parallel and perpendicular dipoles to the total emission. Inspecting Fig. 6, it is observed that at low thicknesses the parallel contribution drops to negligible values in a way compatible with the experimental results. Thus, it is proposed that at low distances from the surface the distribution of dipoles is preferently parallel. This can be rationalized considering that in the electropolymerization the first layers of PANI are near the surface and interacting strongly with it, thus the polymer chains will be adsorbed and oriented parallel to the surface (the emitting dipole is expected to be parallel to the aromatic ring). It has been experimentally observed (see for example [45]) that the first layers of PANI films electrochemically grown are compact and at a certain distance the structure becomes more open and fibrous. As the film grows, the following polymer layers will be more randomly oriented and consequently the emission will have contributions from both parallel and perpendicular orientations. Thus, the total emission (or apparent quantum yield) $q_{a,tot}$ of a film of thickness L is assumed to be given by:
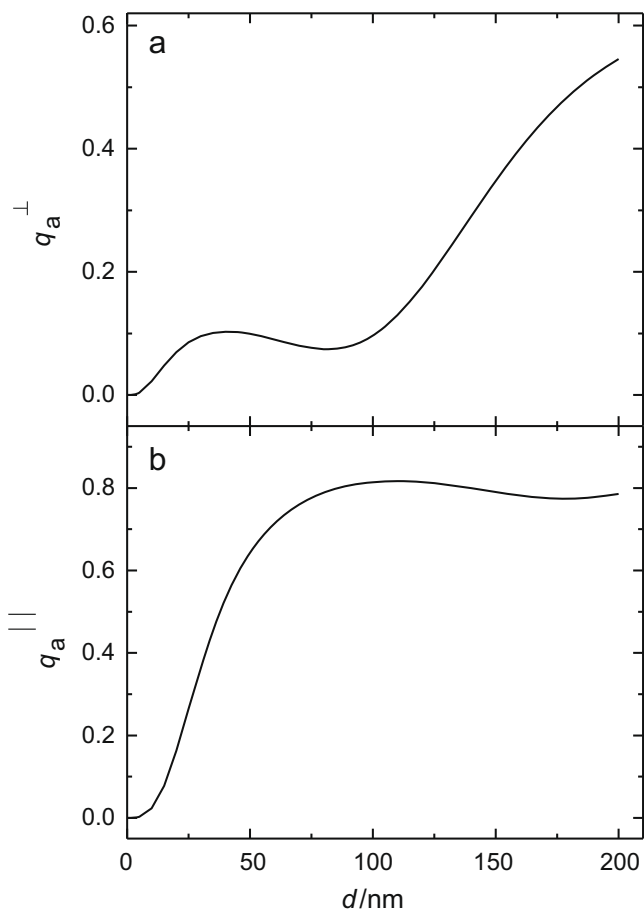
Fig. 6. Apparent quantum yield of PANI molecules on Pt surfaces at λ = 500 nm as a function of distance to the surface: (a) perpendicular and (b) parallel dipoles.

$$q_{a,tot} = \int_0^L [q_a^\perp(d) f_\perp(d) + q_a^\parallel(d)(1 - f_\perp(d))] \mathrm{d}d \tag{21}$$

where $f_\perp(d)$ is the fraction of emitting dipoles which are perpendicular to the surface at the distance d. This function could be in principle deduced from statistical mechanics considerations introducing a polymer/surface interaction with a given distance dependence. However, that procedure requires a detailed knowledge of the microscopic energy contributions in the polymer film, obviously including interaction energies which are not known. For the sake of testing Eq. (21) and its ability to describe the observed behaviour, it was fitted to experimental data with the use of the following sigmoid-like function for f, with two fitting parameters:

$$f_\perp(d) = f_{max}\left(1 - \frac{1}{1 - e^{(d-d_0)/\delta}}\right) \tag{22}$$

where f_{max} corresponds to the f value when $d \to \infty$, d_0 is the d value for the inflection point in the curve and δ is a parameter that defines the slope at that point.

Moreover, to enable the procedure the voltammetric charges Q recorded in the experiments are converted to thicknesses using data from Cruz and Ticianelli [39], for PANI films electropolymerized in H_2SO_4 under similar conditions to those employed here; it is estimated that a 19 mC cm^{-2} film (charge measured between 0.05 and 0.60 V) has a thickness of 200 nm. Fig. 7 shows the fitting of Eq. (21) to the data of Fig. 3a, always at λ_e = 500 nm, normalized by an adjustable parameter in order to scale the experimental intensities to the theoretical range. A good agreement is found. The inset in Fig. 7 shows the $f_\perp(d)$ function resulting. It predicts that in the surface vicinity almost all dipoles are parallel to the sur-
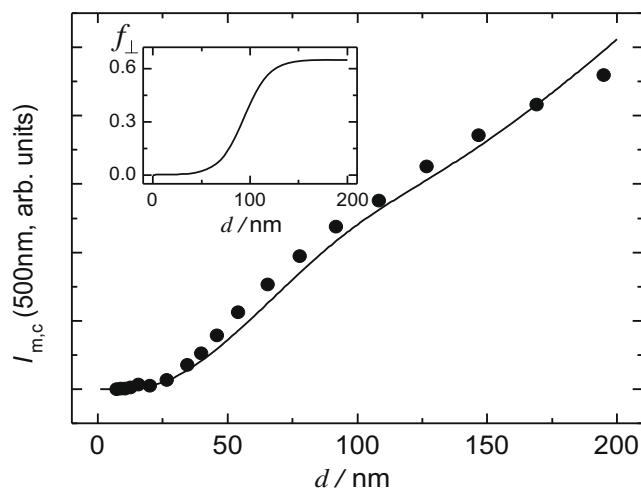

Fig. 7. Corrected emission intensity as a function of thickness at 500 nm (circles) and fitting to Eq. (21) (line) for PANI on Pt. Inset: Fraction of perpendicular dipoles as a function of distance to the surface resulting from the fitting.

face, and as the distance increases the fraction of perpendicular dipoles increases reaching a limiting value, f_{max}, of about 0.6, somewhat higher than 0.5, which would be expected for a random distribution. The transition between the two limits occurs at a distance, d_0, from the surface estimated as ca. 90 nm. Thus, the treatment of Chance et al. [42] is consistent with our experimental results.

4. Conclusions

The fluorescence emission of PANI films supported on metallic surfaces (like Pt) is quenched at low thicknesses. Beyond a critical thickness, the intensity increases sharply. In the case of films supported on non-metallic conducting surfaces (like FTO), the corrected emission intensity shows a monotonous increment with the film thickness, due to the increase in the number of fluorophores. The metallic surface produces the reflection of the emitting molecular dipole field and the fluorescence quenching due to the interaction between the reflected and emitted field. The quantitative analysis of the emission of films supported on metals is consistent with a distribution of emitting dipoles: in the first layers, they are oriented parallel to the electrode surface and then, as the film grows, there is a transition to a contribution of both orientations.

Acknowledgements

References

[1] G.P. Evans, in: H. Gerischer, C.H. Tobías (Eds.), Advances in Electrochemical Science and Engineering, vol. 1, VCH, New York, 1990.
[2] E. Samuelsen (Ed.), Science and Applications of Conducting Polymers, Hilger, Bristol, UK, 1991.
[3] G. Inzelt (Ed.)A.J. Bard (Ed.), Electroanalytical Chemistry, vol. 18, Marcel Dekker, New York, 1994, p. 89.
[4] P.G. Pickup, in: R.E. White (Ed.), Modern Aspects of Electrochemistry, vol. 33, Kluwer Academic Publishers., Plenum Press, New York, 1999, p. 549.
[5] P. Chandrasekhar, in: Conducting Polymers and Applications, Kluwer Academic Publishers, Boston, MA, 1999.

[6] O.S. Wolfbeis, Anal. Chem. 74 (2002) 2663–2678.
[7] S. Christie, E. Scorsone, K. Persaud, F. Kvasnik, Sensor Actuat. B 90 (2003) 163–169.
[8] L.-M. Huang, C.-H. Chem, T.-C. Wen, Electrochim. Acta 51 (2006) 5858.
[9] E. Faulques, V.G. Ivanov, G. Jonusauskas, H. Athalin, O. Pyshkin, J. Wéry, F. Massuyeau, S. Lefrant, Phys. Rev. B 74 (2006) 075202.
[10] A. Sergawie, T. Yahnnes, S. Günes, H. Neugebauer, N.S. Sariciftci, J. Braz. Chem. Soc. 18 (2007) 1189.
[11] X. Yu, Y. Li, N. Zhu, Q. Yang, K. Kalantar-zadeh, Nanotechnology 18 (2007) 015201.
[12] H. Goto, J. Polym. Sci. A: Polym. Chem. 45 (2007) 2065.
[13] J. Zhang, H. Feng, W. Hao, T. Wang, Ceram. Int. 33 (2007) 785.
[14] Y. Son, H.H. Patterson, C.M. Carlin, Chem. Phys. Lett. 162 (1989) 461–466.
[15] J.R.G. Thorne, J.G. Masters, S.A. Williams, A.G. MacDiarmid, R.M. Hochstrasser, Synth. Met. 49 (1992) 159–165.
[16] M.K. Ram, G. Mascetti, S. Paddeu, E. Maccioni, C. Nicolini, Synth. Met. 89 (1997) 63–69.
[17] J.Y. Shimano, A.G. MacDiarmid, Synth. Met. 123 (2001) 251–262.
[18] E.M. Genies, C.T. Tsintavis, J. Electroanal. Chem. 195 (1985) 109–128.
[19] W. Huang, B. Humphrey, A. MacDiarmid, J. Chem. Soc., Faraday Trans. I 82 (1986) 2385–2400.
[20] D. Orata, D.A. Buttry, J. Am. Chem. Soc. 109 (1987) 3574–3581.
[21] G. Horanyi, G. Inzelt, Electrochim. Acta 33 (1988) 947–952.
[22] M.C. Miras, C. Barbero, R. Kötz, O. Hass, J. Electroanal. Chem. 369 (1994) 193–197.
[23] E.M. Andrade, F.V. Molina, M.I. Florit, D. Posadas, J. Electroanal. Chem. 419 (1996) 15–21.
[24] G. Inzelt, Electrochim. Acta 45 (2000) 3865–3876.
[25] S.H. Glarum, J.H. Marshall, J. Electrochem. Soc. 134 (1987) 2160–2165.
[26] R. Patil, Y. Harima, K. Yamashita, K. Komaguchi, Y. Itagaki, M. Shiotani, J. Electroanal. Chem. 518 (2002) 13–19.
[27] A. Petr, A. Neudeck, L. Dunsch, Chem. Phys. Lett. 401 (2005) 130–134.
[28] L. Lizarraga, E.M. Andrade, M.I. Florit, F.V. Molina, J. Phys. Chem. B 109 (2005) 18815–18821.
[29] D. Posadas, M. Fonticelli, M.J. Rodriguez Presa, M.I. Florit, J. Phys. Chem. B 105 (2001) 2291–2296.
[30] D. Posadas, M.J. Rodriguez Presa, M.I. Florit, Electrochim. Acta 46 (2001) 4075–4081.
[31] D. Posadas, M.I. Florit, J. Phys. Chem. B 108 (2004) 15470–15476.
[32] J. Joo, S.M. Long, J.P. Pouget, E.J. Oh, A.G. MacDiarmid, A.J. Epstein, Phys. Rev. B 57 (1998) 9567–9580.
[33] C.-G. Wu, S.-S. Chang, J. Phys. Chem. B 109 (2005) 825–832.
[34] V.I. Krinichnyi, S.V. Tokarev, H.-K. Roth, M. Schrödner, B. Wessling, Synth. Met. 152 (2005) 165–168.
[35] V.N. Prigodin, A.J. Epstein, Europhys. Lett. 60 (5) (2002) 750–756.
[36] P.S. Antonel, E.M. Andrade, F.V. Molina, Electrochim. Acta 49 (2004) 3687–3692.
[37] P.S. Antonel, F.V. Molina, E.M. Andrade, J. Electroanal. Chem. 599 (2007) 52–58.
[38] G.G. Guilbault, in: G.G. Guilbault (Ed.), Practical Fluorescence, second ed., Marcel Dekker, New York, 1990, pp. 1–40.
[39] C.M.G.S. Cruz, E.A. Ticianelli, J. Electroanal. Chem. 428 (1997) 185–192.
[40] K.H. Drexhage, in: E. Wolf (Ed.), Progress in Optics XII, North-Holland, Amsterdam, 1974, p. 165.
[41] R.R. Chance, A. Prock, R. Silbey, J. Chem. Phys. 60 (1974) 2184–2185.
[42] R.R. Chance, A. Prock, R. Silbey, Molecular fluorescence and energy transfer near interfaces, in: I. Progogine, S.A. Rice (Eds.), Advances in Chemical Physics, vol. 37, Wiley, New York, 1978, pp. 1–65.
[43] H. Morawitz, Phys. Rev. 187 (1969) 1792–1796.
[44] M.R. Philpott, J. Chem. Phys. 62 (1975) 1812–1817.
[45] M.J. Rodriguez Presa, H.L. Bandey, R.I. Tucceri, M.I. Florit, D. Posadas, A.R. Hillman, Electrochim. Acta 44 (1999) 2073–2085.